

NASA-CR-205095

Achieving zero current for polar wind outflow on open flux tubes subjected to large photoelectron fluxes

G. R. Wilson¹, G. Khazanov

Space Science Laboratory, NASA/MSFC, Huntsville, AL

J. L. Horwitz

Center for Space Plasma Aeronomic and Astrophysics Research, The University of Alabama in Huntsville

Abstract. In this study we investigate how the condition of zero current on open flux tubes with polar wind outflow, subjected to large photoelectron fluxes, can be achieved. We employ a steady state collisionless semikinetic model to determine the density profiles of O^+ , H^+ , thermal electrons and photoelectrons coming from the ionosphere along with H^+ , ions and electrons coming from the magnetosphere. The model solution attains a potential distribution which both satisfies the condition of charge neutrality and zero current. For the range of parameters considered in this study we find that a 45–60 volt discontinuous potential drop may develop to reflect most of the photoelectrons back toward the ionosphere. This develops because the downward flux of electrons from the magnetosphere to the ionosphere on typical open flux tubes (e.g. the polar rain) appears to be insufficient to balance the photoelectron flux from the ionosphere.

Introduction

Photoelectrons are produced in the upper atmosphere during the ionization of neutral species by solar EUV radiation. They have long been suspected of playing a role in determining or moderating the polar wind [Axford, 1968; Lemaire and Scherer, 1972]. Because of their high energies (~ 20 eV), many of them are able to freely flow along magnetic field lines out of the ionosphere. The typical escape flux of these electrons ranges from 10^9 cm⁻² s⁻¹ (at solar minimum) to 6×10^9 cm⁻² s⁻¹ (at solar maximum). These values come from a two stream phototelectron model [Richards *et al.*, 1994] which includes all of the relevant ionospheric processes involved in the production and transport of the photoelectrons, and has been extensively calibrated against AE and DE photoelectron measurements. Such fluxes represent a current density, at the source altitude, of $1.6 \mu\text{A}/\text{m}^2$ to $9.6 \mu\text{A}/\text{m}^2$ respectively. These currents are comparable to those seen on field lines in the auroral zone. Since many noncurrent-carrying field lines have such photoelectron fluxes on them the plasma must adjust itself in some way so that a large current does not develop. How is zero current flow achieved?

On closed flux tubes zero current could be achieved by a balance between outflowing photoelectrons and photoelectrons from the conjugate ionosphere. If such conjugate fluxes are

unequal then thermal electrons might be forced to flow in the opposite direction from one ionosphere to the other. Such forced inflow of the thermal electrons could heat them, due to adiabatic compression, and modify the ionosphere to generate ion outflows, if compressional heating dominated heatflow.

On open field lines, how the plasma distribution achieves zero current is a more difficult question. Several possibilities may be proposed:

1. The ions in the ionosphere could be accelerated outward by a potential drop so that they produce upflowing fluxes comparable to those of the photoelectrons. Since these fluxes exceed the hydrogen limiting flux the O^+ ions would be required to carry the bulk of such ion flux. This appears to be the conceptual nature of the solution in Tam *et al.* [1995].

2. High altitude thermal electrons ($< \text{few eV}$) could be drawn down the field line as in the hypothesized closed field line case. It is unknown if such electrons exists in large numbers.

3. Magnetospheric electrons ($> \text{few eV}$) could be drawn down the field line to balance the photoelectron flux. Typical polar rain fluxes in the topside ionosphere are only $10^7 - 10^8$ cm⁻² s⁻¹ however, (Winningham and Heikkila [1974]) which appears to be insufficient.

4. A potential barrier could develop that reflects most of the photoelectrons back to the ionosphere. This, in principle, could be in the form of a narrow shock like structure [Barakat and Schunk, 1984].

Evidence Supporting the Existence of a Potential Barrier

We explore here the last of these possibilities, namely that zero current is primarily achieved on open polar cap field lines through the development of a potential barrier that prevents the outflow of most of the photoelectrons. This is supported by LAPI observations of downflowing photoelectrons with energies up to 60 eV (or more) seen in the polar cap at altitudes below 1000 km (Winningham and Gurgiolo [1982]; Pollock *et al.* [1991]; Horwitz *et al.* [1992]), and by the observations of high speed ion beams seen on dayside polar cap field lines at high altitudes by the RIMS instrument on DE-1 (Pollock *et al.* [1991]; Horwitz *et al.* [1992]). The stronger of these two pieces of evidence is the observation of reflected photoelectrons since the relationship between the ion beams and the photoelectrons is not conclusively established.

If such a potential barrier forms and may be considered localized, where would it be expected to develop? This barrier likely forms at altitudes well above the topside ionosphere for the following reasons. 1) The average flow speeds of the O^+ and H^+ ions in the polar cap at altitudes $\leq 1 R_E$ do not show any evidence

¹On leave from the Department of Physics, University of Alabama in Huntsville.

of large potential differences (5 volts or more) between the F region and an altitude of $1 R_E$ (Chandler *et al.* [1991]; Abe *et al.* [1993]). 2) A collisional, semikinetic, transition region model (Wilson [1992], Wilson *et al.* [1996]), which does not include any flow enhancing effects that might be attributable to photoelectrons, predicts H^+ flow speeds that are about a factor of 2 larger than the average observed below $1 R_E$ altitude. Since results from this model are not driven by the boundary conditions and the model is not subject to sonic or heatflow singularities as are steady state generalized transport models, the difference between model results and data strongly suggest the operation of an additional drag force acting on the H^+ . If photoelectrons are a strong accelerator of outflowing ions the disparity between model results and data is greatly compounded. 3) The downflowing photoelectrons seen by the DE2/LAPI instrument show highly spatially structured characteristics even when the upflowing photoelectrons are stable over large distances [Winningham and Gurgiolo, 1982]. This may indicate the larger spatial structure of the distant magnetospheric region where these electrons are reflected or it may indicate the highly dynamic or unstable nature of the reflection process.

Description of the Model

The results presented in this paper were found with a steady state model which determines density profiles of the various species using the collisionless semikinetic treatment. In this

method one can find an expression for the density of a given species as a function of position along the field line and the local value of the electric potential. The expressions derived for this paper assumed that the potential was zero at the lower boundary and decreased monotonically to the upper boundary (i.e. no trapping zones). The velocity distribution of all species at their respective boundaries for in going particles was assumed to be the appropriate half of an isotropic Maxwellian. The one exception was the photoelectron distribution which had a cutoff at 60 eV [Lee *et al.*, 1980]. The ionospheric thermal electrons were assumed to be Boltzmann distributed. The assumption of Maxwellian velocity distributions for particles entering the model domain does not mean that the velocity distributions remained Maxwellian everywhere. The effects of magnetic folding, electric field acceleration and the loss cone combine to create fairly nonMaxwellian velocity distributions at points along the field line.

The model assumes that all species are collisionless. It can be shown from a mean free path analysis that 97% of the photoelectron flux is carried by photoelectrons with sufficient energy to be collisionless given the densities and temperatures listed below. The thermal electrons will be heated by collisions with the photoelectrons but because of their high thermal conductivity the thermal electron temperature will remain within a few percent of being constant and isotropic. The O^+ ion flux and density profile will be unaffected by self collisions but these ions will be slightly heated by collisions with the thermal

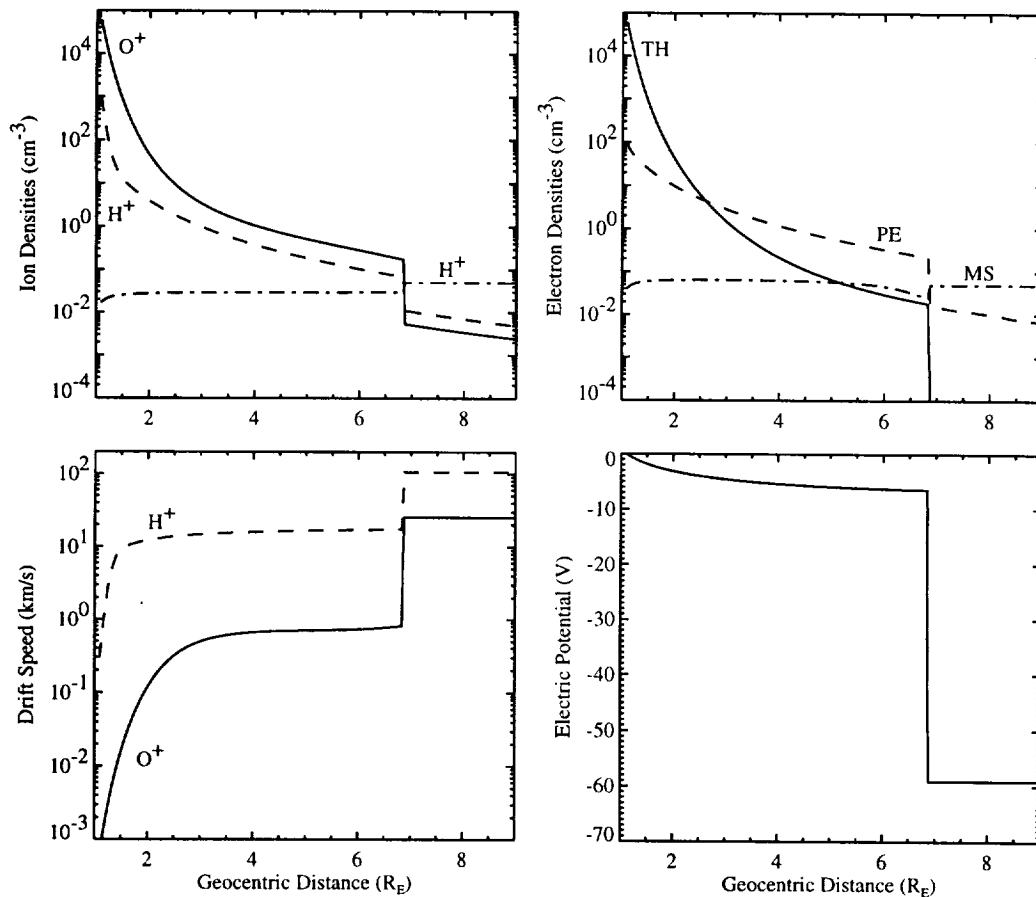


Figure 1. Solar maximum case (with photoelectron upward flux = $6 \times 10^9 \text{ cm}^{-2} \text{ s}^{-1}$ at 500 km) when the mantle plasma density at $9 R_E$ is 0.05 cm^{-3} . The O^+ flux is $3.4 \times 10^6 \text{ cm}^{-2} \text{ s}^{-1}$, the H^+ flux is $2.9 \times 10^7 \text{ cm}^{-2} \text{ s}^{-1}$, the photoelectron flux is $5.1 \times 10^7 \text{ cm}^{-2} \text{ s}^{-1}$ and the polar rain flux is $1.3 \times 10^7 \text{ cm}^{-2} \text{ s}^{-1}$. The combination of these fluxes leaves a residual current of $0.0089 \mu A/m^2$ into the ionosphere.

electrons. This effect is accounted for through adjustment of the boundary O^+ temperature. The one species significantly affected by low altitude collisions is H^+ originating from the ionosphere. To find its density profile we have joined a low altitude collisional semikinetic model profile to that produced by the collisionless semikinetic model, at an altitude where collisions are infrequent.

The parameters used in the cases shown in this paper were: 1) For ionospheric H^+ and O^+ , $T_o = 2000$ K, $N_o(H^+) = 1000$ cm^{-3} , and $N_o(O^+) = 60000$ cm^{-3} . 2) For the thermal electrons $T_e = 5000$ K. 3) For magnetospheric electrons and ions, $kT_o = 100$ eV with N_o ranging between 0.5 and 0.05 cm^{-3} . 4) For the photoelectrons, $kT_{pe} = 20$ eV with N_o ranging between 16.7 and 100.2 cm^{-3} . These values of N_o for the photoelectrons gave upward fluxes, in the absence of any electric potential, of 10^9 to 6×10^9 $cm^{-2} s^{-1}$ representing solar minimum to solar maximum conditions.

To obtain a self consistent solution satisfying zero current and quasineutrality, the code iteratively modifies the electric potential until charge neutrality is achieved. The zero current condition is not directly applied to the iterative calculations but is only incorporated after a solution is found. Because of the transcendental nature of the model, multiple solutions are possible. One such solution involves a small potential drop (\leq a few volts) along the flux tube, with the densities of the ionospheric ions and electrons equal, and separately the magnetospheric ion and electron densities equal. Such a solution

does not produce a zero current because the potential drop along the field line is insufficient to reflect many photoelectrons back to the ionosphere. Another solution produces a large discontinuous drop in the potential. This feature is an electrostatic shock or rarefaction shock that can develop in systems with multiple electron populations that have significantly different temperatures (see *Bezzerrides et al.* [1978] and *Barakat and Schunk.* [1984]). Such class of solutions can satisfy both the conditions of charge neutrality and zero current.

Discussion

Figures 1 and 2 show the results for two different cases with the photoelectron fluxes ranging between the solar minimum and solar maximum values and the magnetospheric plasma densities ranging between 0.05 and 0.5 cm^{-3} . Such range of magnetospheric plasma densities are consistent with the plasma mantle [*Shodhan et al.*, 1996], but are low compared to the magnetosheath [*Sibeck and Gosling*, 1996]. They result in electron fluxes into the ionosphere of 10^7 and 10^8 $cm^{-2} s^{-1}$, consistent with polar rain measurements. In each figure the ion densities are plotted in the first panel, the electron densities in the second, the ionospheric H^+ and O^+ drift speeds in the third and the electric potential in the fourth panel.

The total potential drop between the ionosphere and the magnetosphere in Figure 1 is 59.1 V compared to 47.4 V in Figure 2. This difference is due to the fact that the escaping

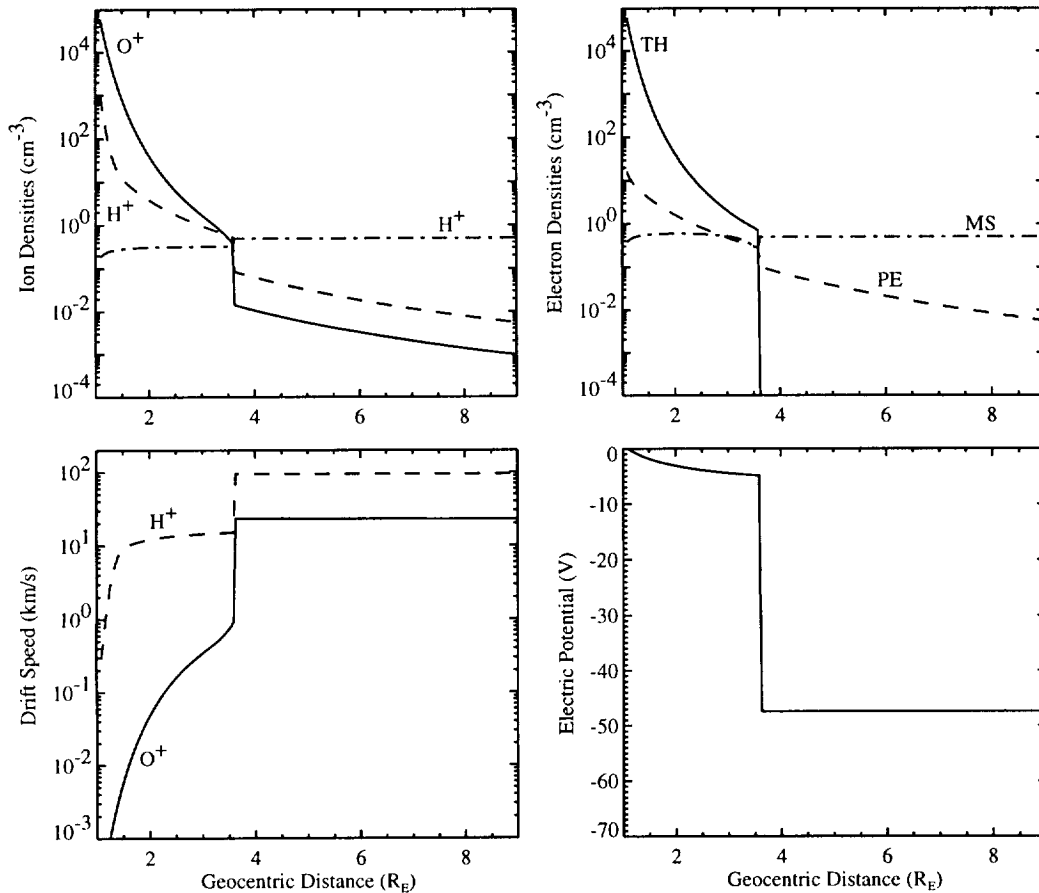


Figure 2. Solar minimum case (with photoelectron upward flux = 10^9 $cm^{-2} s^{-1}$ at 500 km) when the mantle plasma density at 9 R_E is 0.5 cm^{-3} . The O^+ flux is 1.2×10^6 $cm^{-2} s^{-1}$, the H^+ flux is 2.9×10^7 $cm^{-2} s^{-1}$, the photoelectron flux is 1.45×10^8 $cm^{-2} s^{-1}$ and the polar rain flux is 1.23×10^8 $cm^{-2} s^{-1}$. The combination of these fluxes leaves a residual current of 0.013 $\mu A/m^2$ out of the ionosphere.

photoelectron flux is about 600 times greater than the precipitating magnetospheric electron flux for the case in Figure 1 while it is only 10 times greater for the case in Figure 2. An expression that can be used to estimate the potential drop is given in equation (1) where the sum of the ion and electron fluxes is equated to zero (see Knight [1973]).

$$\frac{n_{eo}}{n_{peo}} \sqrt{\frac{T_e}{T_{pe}}} \left(1 - \frac{e\Delta\phi}{kT_e} \right) + \frac{F_i}{n_{peo}} \sqrt{\frac{2\pi m_e}{kT_{pe}}} = \left[\left(1 - \frac{e\Delta\phi}{kT_{pe}} \right) \exp\left(\frac{-e\Delta\phi}{kT_{pe}}\right) - \left(1 + \frac{E_m}{kT_{pe}} \right) \exp\left(\frac{-E_m}{kT_{pe}}\right) \right] \quad (1)$$

In this expression n_{eo} and n_{peo} are the magnetospheric and photoelectron densities at their sources, T_e and T_{pe} are the magnetospheric and photoelectron temperatures respectively, $\Delta\phi$ is the potential drop (assumed to be positive), E_m is the high energy cutoff for the photoelectrons (60 eV), and F_i is the net ion flux along the flux tube. (In the absence of a solution one can use equation (1) to estimate the potential drop by assuming $F_i = 0$.) This equation gives a potential drop of 46.9 V for the solar minimum case (Figure 2) and 59.2 V for the solar maximum case (Figure 1) using the ion fluxes found in those solutions. The results shown in Figures 1 and 2 leave a residual current density of -0.009 and 0.013 $\mu\text{A}/\text{m}^2$ respectively at 500 km altitude.

Unlike the results in Tam *et al.* [1995] (here after referred to as TM) the O^+ fluxes in these cases are relatively small; $3.4 \times 10^6 \text{ cm}^{-2} \text{ s}^{-1}$ for Figure 1 and $1.2 \times 10^6 \text{ cm}^{-2} \text{ s}^{-1}$ for Figure 2 at 500 km altitude. The oxygen ions do not participate much in zeroing the current. If the potential drop which allows attainment of near zero current were to develop at lower altitudes in the topside ionosphere it would not need to be as large as the results presented here since it would accelerated large fluxes of O^+ ions to escape energies so that these could contribute significantly to the current balance. This is the type of solution found in TM. There appears to be two primary choices for a solution that attains zero current on open, photoelectron carrying flux tubes. One is the TM result (and modified versions presented since) and the other is a solution with a high altitude strong photoelectron potential barrier, as presented here. Given that the TM result requires large, near limiting fluxes of O^+ to flow from the sunlit ionosphere and gives supersonic O^+ flows below 1000 km altitude (things which our solution does not give), we feel that our solution is closer to giving the actual effect of photoelectrons on geophysical polar cap flux tubes.

Acknowledgments. The work of G. R. Wilson and J. L. Horwitz was supported in part by NSF grants ATM - 9301024 and ATM - 9402310, and by NASA grant NAGW - 3470 to the University of Alabama in Huntsville. Additional support for G. R. Wilson came from the National Research Council as did the support for G. Khazanov.

References

- Abe, T., B. A. Whalen, A. W. Yau, R. E. Horita, S. Watanabe, and E. Sagawa, EXOS D (Akebono) Suprathermal Mass Spectrometer Observations of the Polar Wind, *J. Geophys. Res.*, **98**, 11191-11203, 1993.
- Axford, W. I., The polar wind and the terrestrial helium budget, *J. Geophys. Res.*, **73**, 6855-6859, 1968.
- Barakat, A. R., and R. W. Schunk, Effect of Hot Electrons on the Polar Wind, *J. Geophys. Res.*, **89**, 9771-9783, 1984.
- Bezzlerides, B., et al., Existence of Rarefaction Shocks in a Laser-Plasma Corona, *Phys. Fluids*, **21**, 2179, 1978.
- Chandler, M. O., J. H. Waite, Jr., and T. E. Moore, Observations of Polar Ion Outflow, *J. Geophys. Res.*, **96**, 1421-1428, 1991.
- Horwitz, J. L., C. J. Pollock, T. E. Moore, W. K. Peterson, J. L. Burch, J. D. Winningham, J. D. Craven, L. A. Frank, and A. Persoon, The Polar Cap Environment of Outflowing O^+ , *J. Geophys. Res.*, **97**, 8361-8379, 1992.
- Knight, S., Parallel electric fields, *Planet. Space Sci.*, **21**, 741-750, 1973.
- Lee, J. S., J. P. Doering, T. A. Potemra, and L. H. Brace, Measurements of the Ambient Photoelectron Spectrum from Atmospheric Explorer: II. AE-E Measurements from 300 to 1000 km During Solar Minimum Conditions, *Planet. Space Sci.*, **28**, 973-996, 1980.
- Lemaire, J., and M. Scherer, The effect of photoelectrons on kinetic polar wind models, *Bull. Cl. Sci. Acad. Roy. Belg.*, **58**, 502, 1972.
- Pollock, C. J., C. R. Chappell, J. L. Horwitz, and J. D. Winningham, Two-Spacecraft Charged Particle Observations Interpreted in Terms of Electrostatic Potential Drops Along Polar Cap Field Lines, in *Modeling Magnetospheric Plasma Processes*, edited by G. R. Wilson, pp. 111-118, Geophys. Mono. #62, AGU, Washington, DC, 1991.
- Richards, P. G., J. A. Fennelly, D. G. Torr, EUVAC: A solar EUV flux model for aeronomic calculations, *J. Geophys. Res.*, **99**, 8981-8992, 1994.
- Shodhan, S., G. L. Siscoe, L. A. Frank, K. L. Ackerson, W. R. Paterson, D. Fairfield, S. Kokubun, and T. Yamamoto, Mantle crossings at Geotail: Comparison with MHD model, *J. Geophys. Res.*, **101**, 153-159, 1996.
- Sibeck, D. G., and J. T. Gosling, Magnetosheath density fluctuations and magnetopause motion, *J. Geophys. Res.*, **101**, 31-40, 1996.
- Tam, S. W. Y., F. Yasseen, and T. Chang, Self-Consistent Kinetic Photoelectron Effects on the Polar Wind, *Geophys. Res. Lett.*, **22**, 2107-2110, 1995.
- Wilson, G. R., Semikinetic Modeling of the Outflow of Ionospheric Plasma Through the Topside Collisional to Collisionless Transition Region, *J. Geophys. Res.*, **97**, 10551-10565, 1992.
- Wilson, G. R., B. L. Giles, M. O. Chandler, Collisional to collisionless ion outflow at the ionosphere-magnetosphere interface, *Adv. Space Res.*, **17**, (10)155-165, 1996.
- Winningham, J. D., and W. J. Heikkila, Polar Cap Auroral Electron Fluxes Observed with Isis 1, *J. Geophys. Res.*, **79**, 949-957, 1974.
- Winningham, J. D., and C. Gurgiolo, DE-2 Photoelectron Measurements Consistent with a Large Scale Parallel Electric Field over the Polar Cap, *Geophys. Res. Lett.*, **9**, 977-979, 1982.
- G. Khazanov and G. R. Wilson, Space Science Laboratory, ES83, NASA/MSFC, Huntsville, AL 35816. (E-mail: wilson@cspar.uah.edu)
- J. L. Horwitz, Center for Space Plasma Aeronomic and Astrophysics Research, EB-136M, The University of Alabama in Huntsville, Huntsville, AL 35899.

(Received October 7, 1996; revised February 4, 1997; accepted March 25, 1997.)